SPACE VECTOR BASED VARIABLE SWITHCHING FREQUENCY PWM ALGORITHMS FOR INDUCTION MOTOR DRIVES WITH REDUCED COMPLEXITY

Kurukunda Ishwarya **Rashmi M R**
Department of Electrical & Electronics Engineering,
Amrita Vishwa Vidyapeetham, School of Engineering, Bangalore, India
ishwaryakurukunda8@gmail.com rashmi.power@gmail.com

Manjunath H V
Professor, Department of Electrical & Electronics Engineering
Amrita Vishwa Vidyapeetham, School of Engineering, Bangalore, India
hv_manjunath@blr.amrita.edu

Abstract: *This paper presents a simple space vector based variable switching frequency PWM algorithm for induction motor drives. The classical space vector approach needs the calculation of angle, sector and reference voltage in each sampling period, which increases the complexity of the PWM algorithm. To reduce the complexity, this paper presents a simple space vector approach in which by using the phase voltages the switching times are calculated in a simple form. By using the proposed approach various switching sequences such as space vector PWM (SVPWM) basic bus-clamping PWM (BBCPWM) and advance bus-clamping PWM (ABCPWM) algorithms are derived. Then, the rms flux ripple which is a measure of current ripple characteristics were plotted for all the sequences. Based on the rms flux ripple characteristics, the zones of superior performance are identified. Then, in each sampling time period, the suitable sequence, which gives reduced flux ripple is applied to the. To validate the proposed algorithm simulation studies have been carried on v/f controlled induction motor drive at various modulation indices and the results are presented. The results show the effectiveness of the proposed work.*

Key words: *ABCPWM, BBCPWM, Induction Motor, SVPWM, VSFPWM.*

1. Introduction

The adjustable speed drives (ASD) are becoming popular in many applications. In order to control the speed of the drive continuously, an ac voltage with controllable magnitude and frequency is required. This required ac voltage can be obtained by using a pulse width modulated voltage source inverter (PWM-VSI). Various PWM algorithms are developed during the fast five decades. A detailed study on various PWM algorithms is presented in [1] and concluded that among the various PWM techniques, the space vector PWM (SVPWM) gives superior waveform quality. In the SVPWM technique, based on the magnitude of the reference voltage and position of the reference voltage vector, the dwelling times of the switching states are calculated [2].

Though, the SVPWM technique gives superior waveform quality, it gives more harmonic distortion at higher modulation indices and also it gives more switching losses of the inverter due to the continuous modulating signal. In the recent years, the basic bus-clamping PWM (BBCPWM) techniques became popular. The BBCPWM techniques give superior waveform quality at higher modulation indices and gives reduced switching losses of the inverter. For the real time implementation of the PWM algorithms, there are two popular approaches namely; triangular comparison (TC) approach and space vector (SV) approach. The correlation between these two approaches is given in [3]. To reduce the complexity involved in the classical SVPWM and BBCPWM algorithms, simple TC approaches are presented in [4-9] by using the concept of voltage magnitude tests and imaginary switching times.

The SVPWM technique divides the zero state time equally among the two possible zero states. But, the BBCPWM algorithms use only one zero state at any time. Thus, by using the freedom in the division of zero state time various PWM algorithms are generated. These can be generated through either TC or SV approach. Recently, advanced bus-clamping PWM (ABCPWM) techniques are attracting many researchers. These ABCPWM algorithms utilize the degrees of freedom in the division of active state. These ABCPWM algorithms can be generated easily through SV approach when compared with the TC approach as explained in [10, 15]. To study the harmonic analysis of various PWM algorithms two approaches are presented in the literature [4-5, 11-14]. Based on the instantaneous current ripple, the rms ripple characteristics can be plotted for each sequence and then the harmonic analysis can be carried out as explained in [11]. Moreover, by using the concept of flux ripple, which is a measure of current ripple, the harmonic analysis can be carried out as explained in [4-5, 12-14].

This paper first reveals a simple space vector approach for the generation of various PWM

techniques such as SVPWM, BBCPWM and ABCPWM algorithms. Then, by utilizing the concept of stator flux ripple, the rms stator flux ripples are plotted, from which finally variable switching frequency PWM (VFSPWM) techniques are presented.

2. Proposed Space Vector Approach

In the classical SV approach, due to involvement of various calculations, the complication in the algorithm increases. To reduce the complexity, a simple SV approach is presented in this paper, in which the dwelling times can be calculated directly from the instantaneous phase voltages. The procedure for the calculation of switching times is as follows:
The instantaneous phase voltages can be given as

$$V_{in} = V_{ref}\cos(\theta - 2(r-1)\pi/3) \text{ for } i=a,b,c \text{ and } r=1,2,3 \quad (1)$$

The maximum, minimum and middle values of V_{in} are calculated in each sampling time period as follows:

$$V_{\max} = \max(V_{in}) \quad (2)$$

$$V_{mid} = mid(V_{in}) \quad (3)$$

$$V_{\min} = \min(V_{in}) \quad (4)$$

Then, the switching dwell times can be calculated as

$$T_1 = \frac{T_s}{V_{dc}}(V_{\max} - V_{mid}) \quad (5)$$

$$T_2 = \frac{T_s}{V_{dc}}(V_{mid} - V_{\min}) \quad (6)$$

$$Tz = T_s - T_1 - T_2 \quad (7)$$

By utilizing the degrees of freedom in the division of zero state and active state times various PWM algorithms such as SVPWM, BBCPWM and ABCPWM techniques can be generated and these are given in Table1.

Table-I PWM Sequences in all six sectors

Sector Number	SVPWM	BBC PWM-1	BBC PWM-2	ABC PWM-1	ABC PWM-2
1	0127-7210	012-210	721-127	0121-1210	7212-2127
2	0327-7230	032-230	723-327	0323-3230	7232-2327
3	0347-7430	034-430	743-347	0343-3430	7434-4347
4	0547-7450	054-450	745-547	0545-5450	7454-4547
5	0567-7650	056-650	765-567	0565-5650	7656-6567
6	0167-7610	016-610	761-167	0161-1610	7616-6167

From Table-1, it can be observed that the number of commutations in each sampling time period for SVPWM and ABCPWM algorithms is three while for BBCPWM algorithms is two. Hence the sampling frequency of the SVPWM and ABCPWM algorithms is the twice the average switching frequency (*fs* = 2**fsw*), whereas the sampling frequency of the BBCPWM algorithms is three times the average switching frequency (*fs* =3**fsw*). The SVPWM and BBCPWM algorithms cannot switch more than once in each T_s. Hence, these can be generated with triangular comparison approach also. But, in ABCPWM algorithms, one of the phases will be clamped to the dc bus while the one of the other phases will switch twice in each T_s. These sequences cannot be generated with triangular comparison approach. These can be generated by using the space vector approach very easily. Thus, the space vector approach offers more degrees of freedom compared to the carrier comparison approach.

3. Proposed VFSPWM Algorithms

A. Analysis of Stator Flux Ripple

The total harmonic distortion (THD) of a line current (I_{THD}) is a widely used measure for the quality of waveform generated by a PWM inverter, which is defined as

$$I_{THD} = \frac{I}{I_1}\sqrt{\sum_{n\neq 1} I_n^2} \quad (8)$$

where, I_1 and I_n are the rms values of the fundamental and the nth harmonic components of the no-load current respectively.

The SV approach generates the reference voltage in an average manner and hence there is always a difference voltage will exists between the applied voltage and reference voltage. This difference voltage is known as ripple voltage vector, which depends on angle and modulation index (M_i). The ripple voltage vectors and trajectory of the stator flux ripple for SVPWM and BBCPWM sequences are shown in Fig. 1. The corresponding d-axis and q-axis components of the stator flux ripple vector are as shown in Fig. 2. Here T_1, T_2, T_0 and T_7 are the switching times of the voltage vectors V_1, V_2, V_0 and V_7. The T_0 and T_7 are taken as $T_0 = kT_z$ and $T_7 = (1-k)T_z$. For k=0.5, 0 and 1, the expressions for SVPWM, BBPWM-1 and BBCPWM-2 techniques can be derived.
The error volt-seconds corresponding to the ripple voltage vectors are as follows:

$$V_{r1}T_1 = \left(\frac{2}{3}V_{dc}\sin\alpha\right)T_1 + j\left(\frac{2}{3}V_{dc}\cos\alpha - V_{ref}\right)T_1 \quad (9)$$

$$V_{r2}T_2 = -\left(\frac{2}{3}V_{dc}\sin\left(60^o - \alpha\right)\right)T_2 + j\left(\frac{2}{3}V_{dc}\cos\left(60^o - \alpha\right) - V_{ref}\right)T_2 \quad (10)$$

$$V_{r0}T_0 = -jV_{ref}T_0 = -j\frac{2M_iV_{dc}}{\pi}T_0 = jQ_0 \quad (11)$$

$$V_{r7}T_7 = -jV_{ref}T_7 = -j\frac{2M_iV_{dc}}{\pi}T_7 = jQ_7 \tag{12}$$

By using the switching times expressions of classical SVPWM technique [4-5], the (9) and (10) can be expressed in terms of switching times as given in (13) - (14).

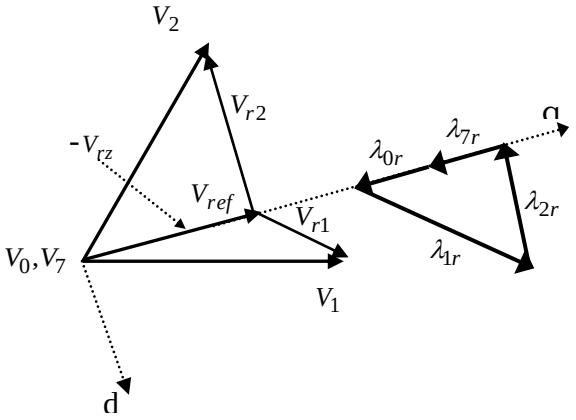

Fig. 1 Voltage ripple vectors and trajectory of the flux ripple

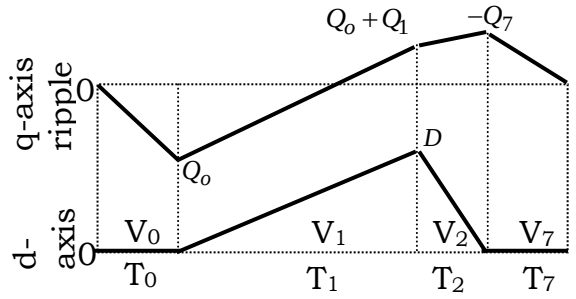

Fig. 2 q-axis and d-axis components of the flux ripple vectors

$$V_{r1}T_1 = \frac{\pi V_{dc}}{3\sqrt{3}M_i}\frac{T_1T_2}{T_s} + j\left(\frac{2V_{dc}\pi(T_1+0.5T_2)}{9M_iT_s} - \frac{2V_{dc}M_i}{\pi}\right)T_1 = D + jQ_1 \tag{13}$$

$$V_{r2}T_2 = -\frac{\pi V_{dc}}{3\sqrt{3}M_i}\frac{T_1T_2}{T_s} + j\left(\frac{2V_{dc}\pi(0.5T_1+T_2)}{9M_iT_s} - \frac{2V_{dc}M_i}{\pi}\right)T_2 = -D + jQ_2 \tag{14}$$

By using the expressions (11) – (14) and Fig 2, the expressions of the rms stator flux ripple can be derived as in (15).

$$\psi^2(rms) = \frac{1}{3T_s}\left\{\begin{array}{l}\frac{4V_{dc}^2M_i^2}{\pi^2}\left(\begin{array}{l}(T_0+T_1)^3 + T_7{}^3 + T_2(T_0^2 \\ + T_1^2 + T_7^2 + 2T_0T_1 - T_1T_7 - T_0T_7)\end{array}\right) \\ + \frac{\pi^2V_{dc}^2}{81M_i^2T_s^2}(4T_1^5 + 8T_1^4T_2 + 8T_1^3T_2{}^2 + 8T_1^2T_2{}^3) \\ - \frac{V_{dc}^2}{9T_s}(8T_1^4 + 12T_1^3T_2 + 12T_1^3T_0 + 14T_1^2T_0T_2 + \\ 4T_0T_1T_2{}^2 + 4T_1^2T_2{}^2 \\ - 4T_1^2T_2T_7 - 2T_7T_1T_2{}^2)\end{array}\right\} \tag{15}$$

Similarly, the harmonic analysis of ABCPWM algorithms can be carried out. The variation of stator flux ripple vectors in case of ABCPWM-I and ABCPWM-II algorithms are shown in Fig. 3 and Fig 5. The corresponding d- and q-axes stator flux ripple trajectories of AZSPWM-1 and AZSPWM-2 are as shown in Fig 4 and Fig 6 respectively. Similar to the SVPWM and BBCPWM algorithms, the rms stator flux ripple expression can be calculated as given in (16) and (17).

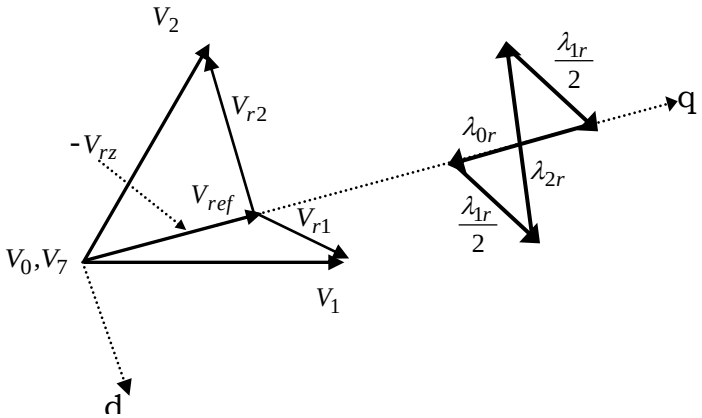

Fig. 3 voltage ripple vectors and trajectory of the flux ripple for ABCPWM-I

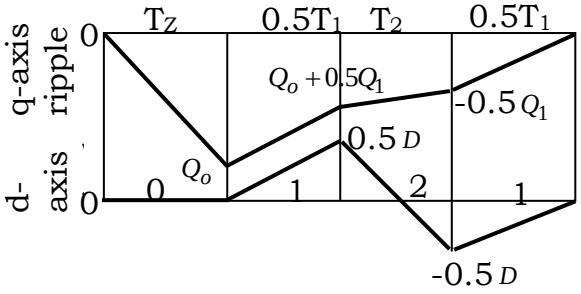

Fig. 4 q-axis and d-axis components of the flux ripple vectors for ABCPWM-I

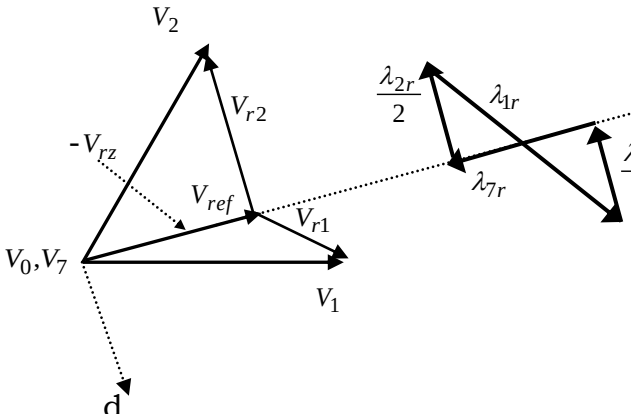

Fig. 5 voltage ripple vectors and trajectory of the flux ripple for ABCPWM-II

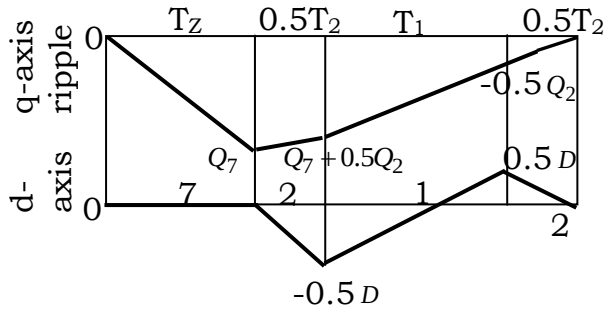

Fig. 6 q- and d-axis components of the flux ripple vectors for ABCPWM-II

$$\psi^2_{(rms),ABCPWM\text{-}I} = \frac{1}{3T_s}\left\{\begin{aligned}&\frac{V_{dc}^2 M_i^2}{\pi^2}(4T_z^3 + 6T_1T_z^2 + 4T_2T_z^2 + 3T_zT_1^2 + \\ &2T_1T_2T_z + T_1^3 + T_2T_1^2) \\ &+\frac{\pi^2 V_{dc}^2}{324M_i^2T_s^2}(4T_1^5 + 8T_1^4T_2 + 8T_1^3T_2^2 + 4T_1^2T_2^3) \\ &-\frac{V_{dc}^2}{9T_s}(3T_1^3T_z + \frac{7}{2}T_1^2T_zT_2 + T_zT_1T_2^2 + 2T_1^4 + \\ &3T_1^3T_2 + T_1^2T_2^2)\end{aligned}\right\} \quad (16)$$

$$\psi^2_{(rms),ABCPWM\text{-}II} = \frac{1}{3T_s}\left\{\begin{aligned}&\frac{V_{dc}^2 M_i^2}{\pi^2}(4T_z^3 + 6T_2T_z^2 + 4T_1T_z^2 + 3T_zT_2^2 + \\ &2T_1T_2T_z + T_2^3 + T_1T_2^2) \\ &+\frac{\pi^2 V_{dc}^2}{324M_i^2T_s^2}(4T_2^5 + 8T_2^4T_1 + 8T_2^3T_1^2 + 4T_2^2T_1^3) \\ &-\frac{V_{dc}^2}{9T_s}(3T_2^3T_z + \frac{7}{2}T_2^2T_zT_1 + T_zT_2T_1^2 + 2T_2^4 + \\ &3T_2^3T_1 + T_1^2T_2^2)\end{aligned}\right\} \quad (17)$$

Thus, the rms stator flux ripple characteristics can be obtained for all the switching sequences. The current pulsations mainly dependent on both d- and q-axes flux ripples and the torque pulsation depends on q-axis flux ripple only.

B. Proposed VFCPWM Algorithms

To achieve better waveform quality, the harmonic distortion must be reduced. To achieve lower THD, the rms flux ripple must be low. The rms stator flux ripple characteristics of SVPWM, BBCPWM and ABCPWM algorithms can be plotted as shown in Fig. 7 – Fig. 11 at different modulation indices. From Fig. 7 – Fig. 11, the following points can be concluded:

- Replacing α by $(60^o - \alpha)$ in the rms stator flux ripple expressions of SVPWM does not change its value, which can be given as in (18).

$$\psi^2_{(rms)SVPWM}(\alpha) = \psi^2_{(rms)SVPWM}(60^o - \alpha) \quad (18)$$

- Swapping of T_1 and T_2 and that of Q_1 and Q_2, in the rms stator flux ripple expression of BBCPWM-1 (ABCPWM-1) lead to the rms stator flux ripple expression of BBCPWM-II (ABCPWM-2) as given in (19) and (20).

$$\psi^2_{(rms)BBCPWM\text{-}1}(\alpha) = \psi^2_{(rms)BBCPWM\text{-}2}(60^o - \alpha) \quad (19)$$

$$\psi^2_{(rms)ABCPWM\text{-}1}(\alpha) = \psi^2_{(rms)ABCPWM\text{-}2}(60^o - \alpha) \quad (20)$$

- Moreover, from Fig. 7 - Fig. 11, it can be concluded that at lower modulation indices, the SVPWM algorithm gives superior performance whereas at medium modulation indices BBCPWM algorithms give superior performance and at higher modulation indices the ABCPWM algorithms give superior performance.

To minimize the harmonic distortion in the line current, the rms current ripple or rms stator flux ripple over every sampling time period should be reduced. The proposed variable switching frequency PWM (VFSPWM) algorithms employ the best sequence out of the considered possible sequences to minimize the rms current ripple in each sampling time period. The development of proposed VFSPWM techniques for reduced current ripple involves determination of superior performance for every sequence. The zone of superior performance for a given sequence is the spatial zone within a sector where the given sequence results in less mean square stator flux ripple than the other sequences considered. By taking the combination of different sequences two types of VFSPWM algorithms are generated as follows:

- 3-zone VFSPWM algorithm
- 5-zone VFSPWM algorithm

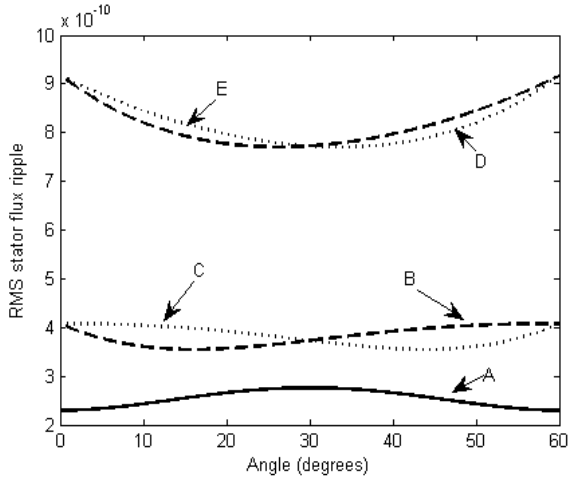

Fig. 7 Variation of stator flux ripple over the first sector for $M_i = 0.4$ (A: SVPWM, B: BBCPWM-1, C: BBCPWM-2, D: ABCPWM-1 and E: ABCPWM-2)

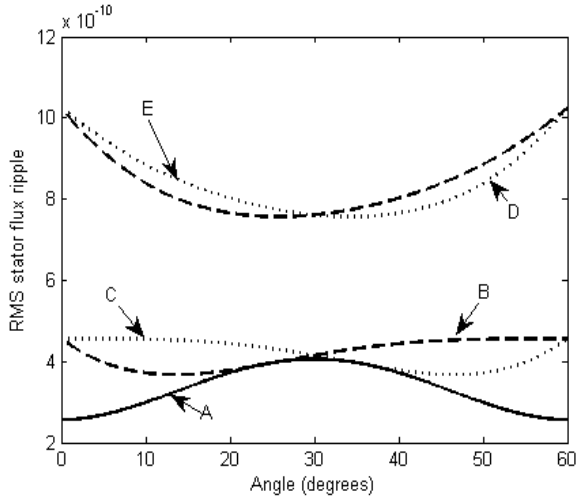

Fig. 8 Variation of stator flux ripple over the first sector for $M_i = 0.55$ (A: SVPWM, B: BBCPWM-1, C: BBCPWM-2, D: ABCPWM-1 and E: ABCPWM-2)

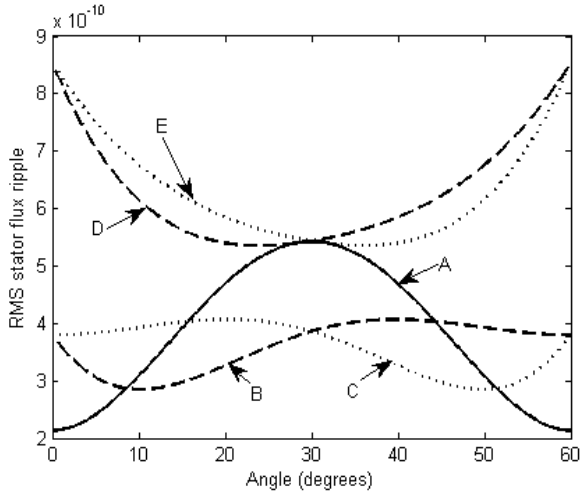

Fig. 9 Variation of stator flux ripple over the first sector for $M_i = 0.68$ (A: SVPWM, B: BBCPWM-1, C: BBCPWM-2, D: ABCPWM-1 and E: ABCPWM-2)

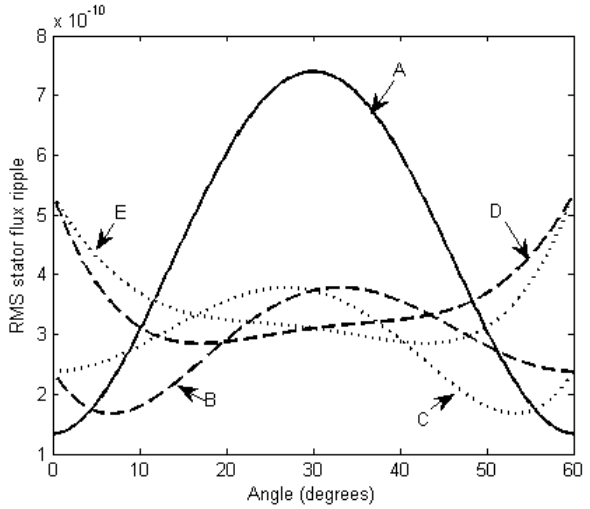

Fig. 10 Variation of stator flux ripple over the first sector for $M_i = 0.8$ (A: SVPWM, B: BBCPWM-1, C: BBCPWM-2, D: ABCPWM-1 and E: ABCPWM-2)

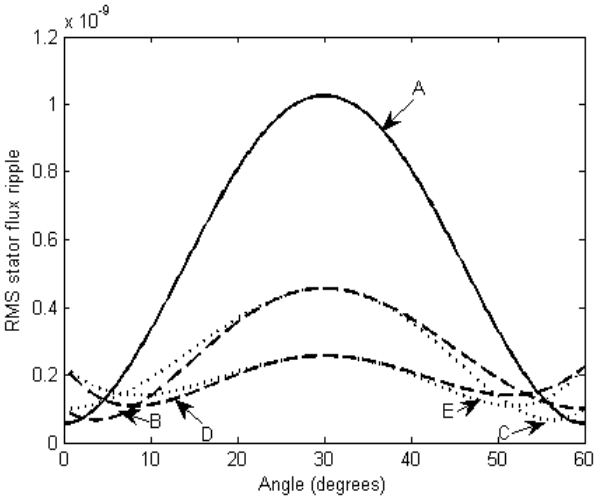

Fig. 11 Variation of stator flux ripple over the first sector for $M_i = 0.906$ (A: SVPWM, B: BBCPWM-1, C: BBCPWM-2, D: ABCPWM-1 and E: ABCPWM-2)

The 3-zone VSFPWM technique involves the use of switching sequences 0127, 012 and 721. From Fig. 7 – Fig. 11, the zones of superior performance of 0127, 012 and 721 sequences can be identified as shown in Fig. 12. Similarly, for the 5-zone VSFPWM algorithm, the zones of superior performance can be represented as shown in Fig. 13, which uses all five switching sequences.

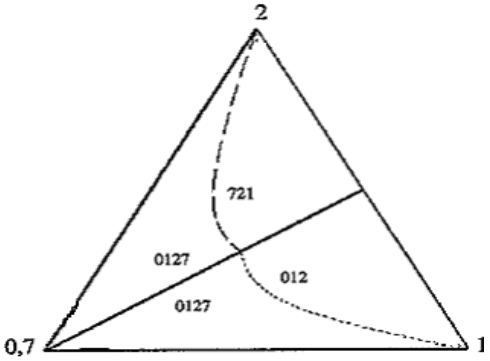

Fig. 12 3-zone VFSPWM Algorithm

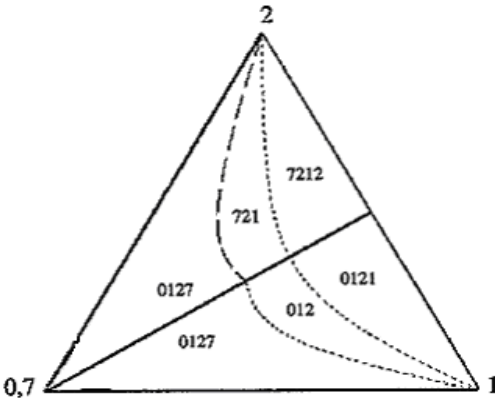

Fig. 13 5-zone VFSPWM Algorithm

4. Simulation Results and Discussion

To validate the proposed space vector based VSFPWM algorithms, the simulation studies have been carried out on v/f controlled induction motor drive. For the simulation studies, the average switching frequency is taken as 3 kHz and dc link voltage is taken as 540V. The simulation studies are carried out at different operating frequencies (modulation indices). The simulation results of SVPWM and proposed VSFPWM algorithms are as shown in Fig. 14 – Fig. 28 at various modulation indices.

From the simulation results, it can be concluded that the proposed VSFPWM algorithms give superior performance when compared with the SVPWM algorithm. As the proposed VSFPWM algorithms use the bus-clamping sequences, the switching losses of the inverter can be decreased. Moreover, the proposed VSFPWM algorithms give spread spectra and also give reduced harmonic amplitudes at the multiples of switching frequencies when compared with the SVPWM algorithm. This leads to the reduction of acoustic noise.

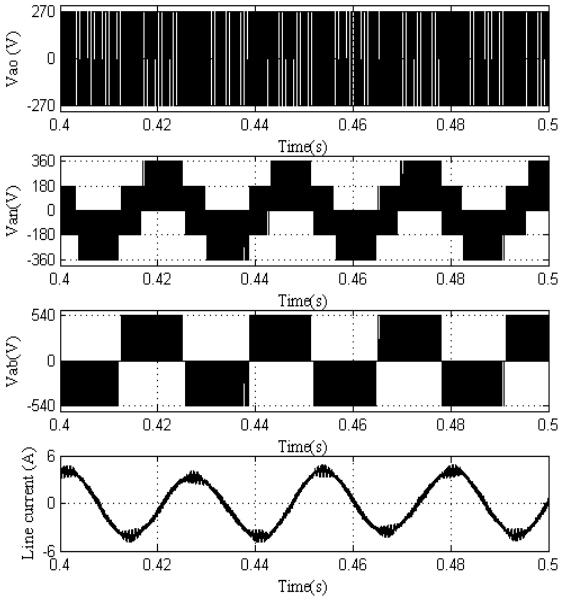

Fig.14 Simulation results for SVPWM based induction motor drive at M_i=0.69

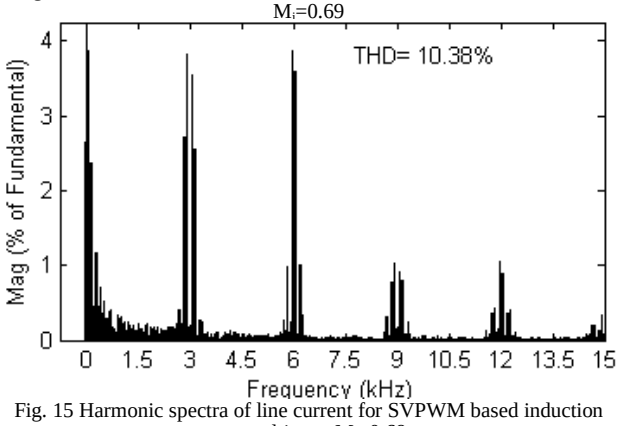

Fig. 15 Harmonic spectra of line current for SVPWM based induction motor drive at M_i=0.69

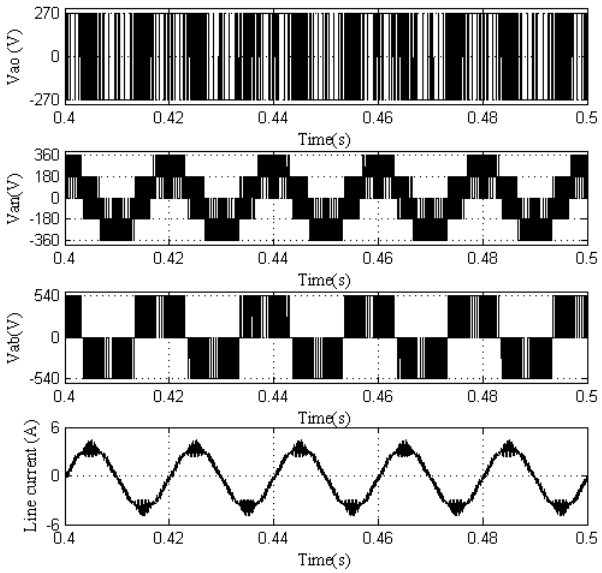

Fig. 16 Simulation results for SVPWM based induction motor drive at M_i=0.906

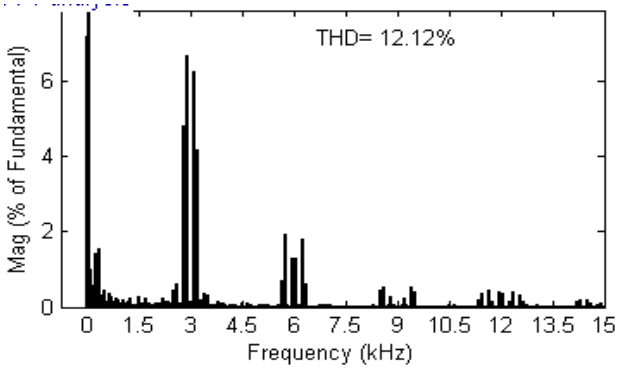

Fig. 17 Harmonic spectra of line current for SVPWM based induction motor drive at M_i=0.906

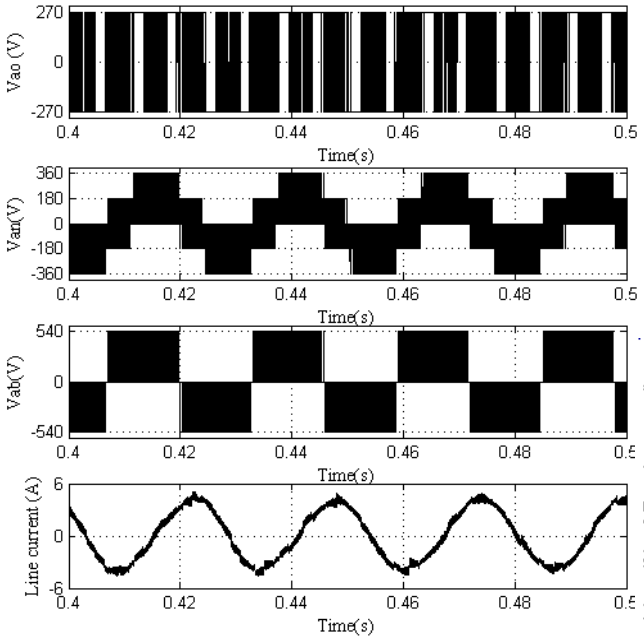

Fig 18 Simulation results for 3-zone VSFPWM based induction motor drive at M_i=0.69

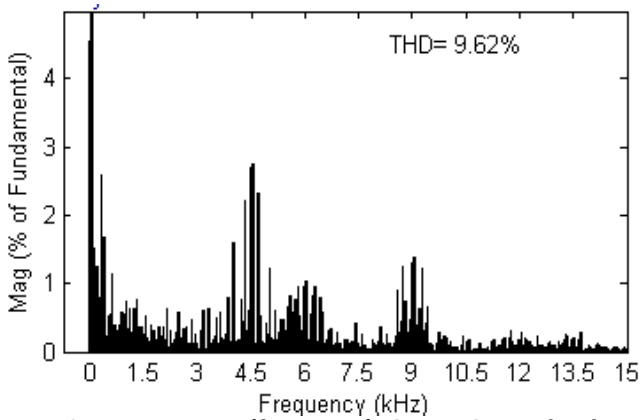

Fig. 19 Harmonic spectra of line current for 3-zone VSFPWM based induction motor drive at M_i=0.69

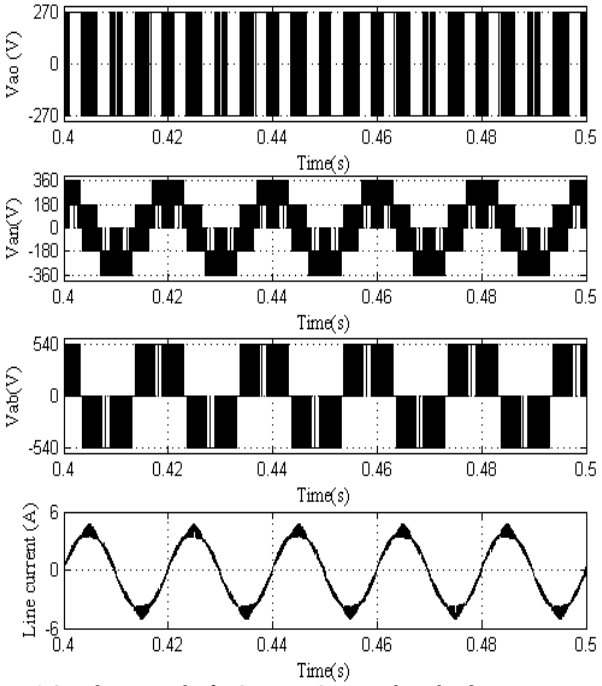

Fig 20 Simulation results for 3-zone VSFPWM based induction motor drive at M_i=0.906

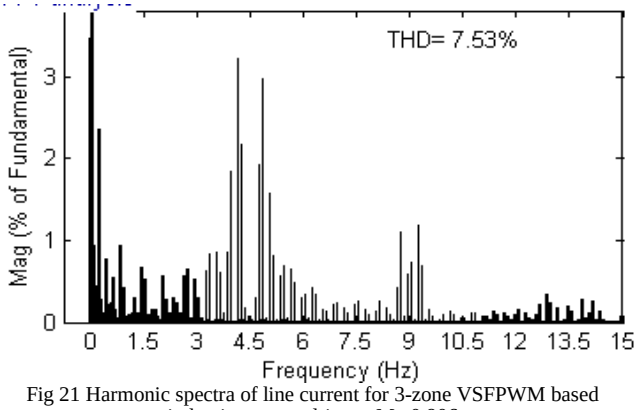

Fig 21 Harmonic spectra of line current for 3-zone VSFPWM based induction motor drive at M_i=0.906

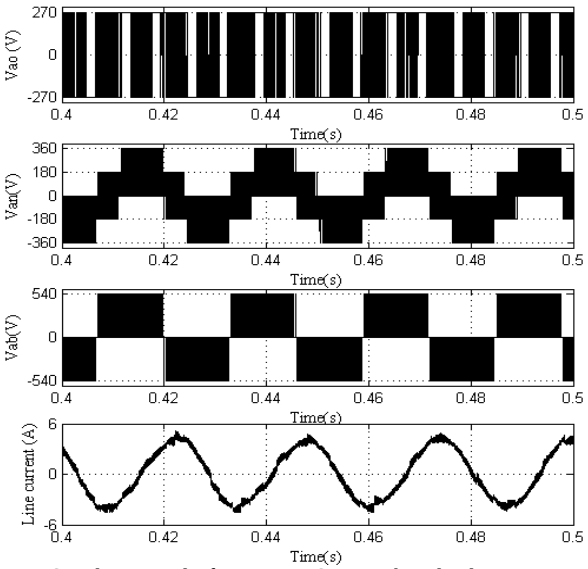

Fig 22 Simulation results for 5-zone VSFPWM based induction motor drive at M_i=0.69

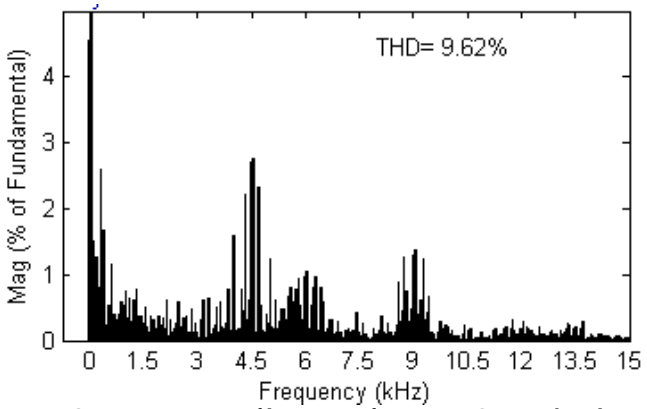

Fig. 23 Harmonic spectra of line current for 5-zone VSFPWM based induction motor drive at M_i=0.69

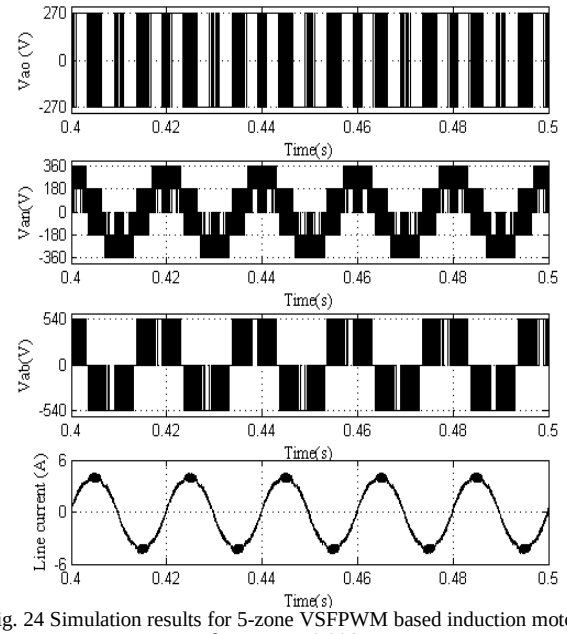

Fig. 24 Simulation results for 5-zone VSFPWM based induction motor drive at M_i=0.906

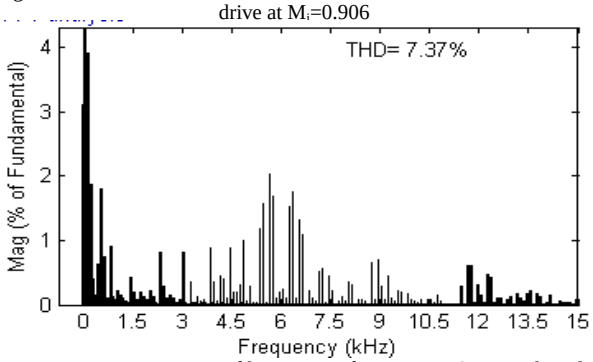

Fig. 25 Harmonic spectra of line current for 5-zone VSFPWM based induction motor drive at M_i=0.906

The spectral density results for SVPWM and proposed VSFPWM algorithms are shown in Fig. 26 – Fig. 27. From these, it can be observed that the proposed VSFPWM algorithms will give reduced acoustical noise of the drive system.

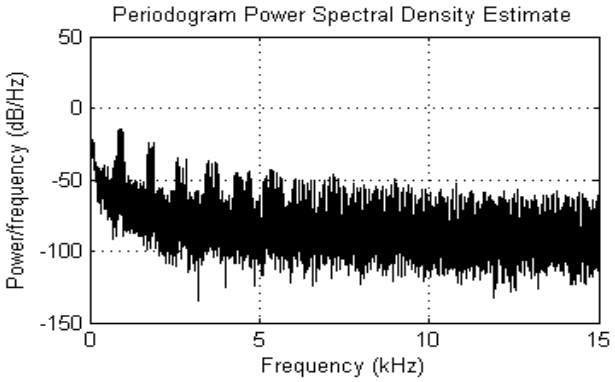

Fig. 26 Power spectrum of the-line current with the SVPWM algorithm

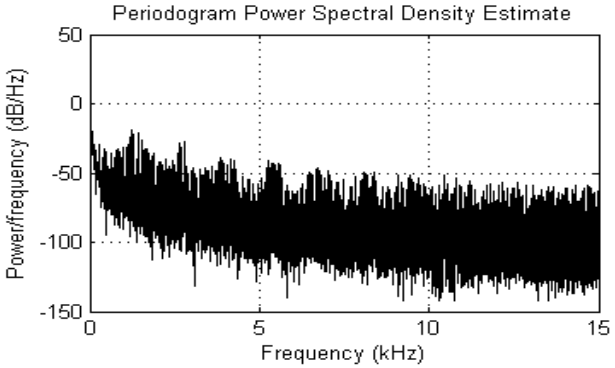

Fig. 27 Power spectrum of the-line current with the VSFPWM1 algorithm

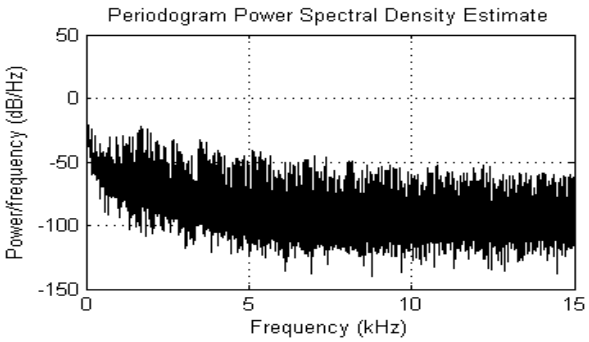

Fig. 28 Power spectrum of the line current with the VSFPWM2 algorithm

5. Conclusions

A simple SV approach is presented in this paper, which uses instantaneous phase voltages only for the calculation of switching times of the inverter devices. By using the proposed approach various PWM techniques such as SVPWM, BBCPWM and ABCPWM algorithms are generated. Then, by using the concept of stator flux ripple, the rms flux ripple expressions are derived for all sequences. Based on the magnitude of rms stator flux ripple, a suitable switching sequence, which results in reduced harmonic distortion, is applied in each sampling time interval. Thus, the proposed VSFPWM algorithms use a suitable sequence in each sampling period. From the simulation results, it can be observed that the proposed VSFPWM algorithms will give reduced harmonic distortion and acoustical noise when compared with the SVPWM algorithm.

References

1. Joachim Holtz, "Pulse width modulation – A survey" *IEEE Trans. Ind. Electron*., vol. 39, no. 5, Dec 1992, pp 410-420.
2. Heinz Willi Vander Broeck, Hnas-Christoph Skudelny and Georg Viktor Stanke, "Analysis and realization of a pulse width modulator based on voltage space vectors" *IEEE Trans. Ind. Applicat*., vol. 24, no. 1, Jan/Feb 1988, pp 142-150.
3. Keliang Zhou and Danwei Wang, "Relationship between space-vector modulation and three-phase carrier-based PWM: A comprehensive analysis" *IEEE Trans. Ind. Electron*, vol. 49, no. 1, Feb 2002, pp. 186-196.
4. Ahmet M. Hava, Russel J. Kerkman and Thomas A. Lipo, "A high-performance generalized discontinuous PWM algorithm" *IEEE Trans. Ind. Applicat*., vol. 34, no. 5,Sep/Oct 1998, pp. 1059-1071.
5. Ahmet M. Hava, Russel J. Kerkman and Thomas A. Lipo, "Simple analytical and graphical methods for carrier-based PWM-VSI drives" *IEEE Trans. Power Electron*., vol. 14, no. 1, Jan 1999, pp. 49-61.
6. Dae-Woong Chung, Joohn-Sheok Kim and Seung-Ki Sul, "Unified voltage modulation technique for real-time three-phase power conversion" *IEEE Trans. Ind. Applicat*., vol. 34, no. 2, Mar/Apr 1998, pp. 374-380.
7. Vladimir Blasko, "Analysis of a hybrid PWM based on modified space-vector and triangle-comparison methods" *IEEE Trans. Ind. Applicat*., vol. 33, no. 3, May/Jun 1997, pp. 756-764.
8. Olorunfemi Ojo, "The generalized discontinuous PWM scheme for three-phase voltage source inverters" *IEEE Trans. Ind. Electron*., vol. 51, no. 6, Dec 2004, pp. 1280-1289.
9. Edison Roberto C.Da Silva, Euzeli Cipriano Dos Santos, Jr., and Cursino Brandao Jacobina, "Pulsewidth modulation strategies" *IEEE IE Magazine,* 2011 pp. 37-45.
10. G. Narayanan and V.T. Ranganathan, "Triangle comparison and space vector approaches to pulse width modulation in inverter fed drive", *Journal of Indian Institute of Science,* Sept/Oct 2000, pp. 409-427.
11. Domenico Casadei. Giovanni Serra, Angelo Tani and Luca Zarri, "Theoritical and experimental analysis for the RMS current ripple minimization in induction motor drives controlled by SVM technique" *IEEE Trans. Ind. Electron.*, vol. 51 no. 5, Oct 2004, pp. 1056-1065.
12. G. Narayanan and V.T. Ranganathan, "Analytical evaluation of harmonic distortion in PWM AC drives using the notion of stator flux ripple" *IEEE Trans. Power Electron.*, vol. 20, no. 2, Mar 2005, pp. 466-474.
13. G.Narayanan , Di Zhao, H. Krishnamurthy and Rajapandian Ayyanar, "Space vector based hybrid techniques for reduced current ripple" *IEEE Trans*. *Ind. Applic.*, Vol. 55, No.4,, April 2008, pp.1614-1626.
14. Di Zhao, V. S. S. Pavan Kumar Hari, G. Narayanan "Space Vector Based Hybrid Pulse Width Modulation Techniques for Reduced Harmonic Distortion and Switching Loss" *IEEE Transactions on Power electronics*, vol.25, Issue.4, Mar, 2010, pp.760-774.
15 Kurukunda Ishwarya and Rashmi M R, "Space Vector Based PWM Strategies for VSI Fed Induction Motor Drives with Reduced Complexity " IEEE international conference on 2014 Power And Energy Systems: Towards Sustainable Energy Systems (PESTSE2014), pp.1-8